Indian Journal of Fibre & Textile Research
Vol. 49, March 2024, pp. 27-41
DOI: 10.56042/ijftr.v49i1.9551

Optimisation of fibre denier specific carding parameters to modulate the structure of needle-punched nonwoven

Priyal Dixit & S M Ishtiaque[a]

Department of Textile and Fibre Engineering, Indian Institute of Technology Delhi, New Delhi 110 016, India

Received 30 March 2022; revised received and accepted 16 March 2023

Fibre denier specific carding parameters, such as feeder speed, cylinder speed and doffer speed, have been optimised to modulate the structure of needle-punched nonwoven. Polyester fibres of 3 denier, 4 denier and 6 denier are used to prepare nonwoven fabrics at different carding parameters. Box Behnken three factors three levels factorial design is used to prepare the nonwoven samples. Fibre orientation is measured with the help of Lindsley's and image analysis techniques in terms of indices, like proportion of curved fibre ends, coefficient of relative fibre parallelisation and anisotropy of fibre inclination angle respectively. A non-linear regression technique has been developed to establish a relationship between tortuosity factor and measured values of fibre diameter, proportion of curved fibre ends, coefficient of relative fibre parallelisation, anisotropy of fibre inclination angle and mean flow pore size. The findings show the significance of carding parameters to modulate the orientation of fibres in carded web to enhance the functional properties of needle-punched nonwoven.

Keywords: Carding, Fibre denier, Fibre orientation, Needle-punched nonwoven, Nonwoven fabrics, Tortuosity factor

1 Introduction

The significance of using nonwoven fabrics in filter applications lies in the presence of a wide range of pore sizes and fibre configurations. Filtration performance is mostly measured in terms of pressure drop and filtration efficiency which are primarily regulated by the filter's internal microstructure. Researchers have explored various factors influencing the performance of nonwoven filter media. The importance of punching parameters on nonwoven characteristics has been realised by several researchers[1-3]. Kothari *et al.*[4] investigated the effect of punch density on filtration performance and associated properties in layered nonwoven fabrics. Dixit *et al.*[5] explored the concept of sequential punching in determining the behaviour of layered nonwoven filter fabrics. Chatterjee *et al.*[6-8] studied the influence of various fibre properties on nonwoven fabric performance.

But Lamb *et al.*[9] concluded that fibre geometry plays a crucial role in determining the structure and properties of the nonwoven. Das *et al.*[10] observed that fibre having grooved cross-section provided better filtration with high-pressure drop while vice-versa was noticed with fibres of circular cross-section. Pradhan *et al.*[11] optimally designed nonwoven filter media using fibres of different fineness using response surface methodology. Evidently, earlier studies have mainly focussed on fibre characteristics and punching parameters of nonwoven fabrics as variable to optimise the functional properties of nonwoven. However, much attention has not been paid to realise the importance of fibre orientation in carded web influenced by carding parameters on the functional properties of nonwoven.

The significance of the carding process to regulate the orientation of fibres in the carded web has been very much accepted for improving the spun-yarn quality[12]. Ishtiaque *et al.*[13-14] studied the influence of fibre opening during carding processon yarn regularity and strength. Garde *et al.*[15], Jabbar *et al.*[16], and Neckar and Das[17] studied the influence of the orientation of fibres in the carded web and their relationship with yarn quality. However, to the best of our knowledge the importance of carding parameters in modulating the structure of nonwoven and its influenceon functional properties of fabrics has not been much explored in the literature. However, the relationship between the orientation of fibres and the properties of nonwovens influenced by carding machine parameters has been recently explored by Roy *et al.*[18-20]. To explore better understanding in this direction, the present authors have investigated the

[a]Corresponding author.
E-mail: ishtiaque@iitd.ac.in

orientation of fibres in nonwoven card web using newly proposed structural indices[21] and their relationship with functional properties of nonwoven filter fabric.

Accordingly, in present work, emphasis is laid to realise the significance of studying the structure of carded web influenced by carding parameters of nonwoven fabric. The fibre orientation in the carded web made of fibre of different deniers and different combinations of feeder, cylinder and doffer speedswas measured in terms of proportion of curved fibre ends, coefficient of relative fibre parallelisation, anisotropy of inclination angle of fibres, and tortuosity factor in nonwoven fabrics. A nonlinear regression equation was developed to establish the relationship between the tortuosity factor and measured structural characteristics, fibre diameter, and mean flow pore size. The proposed study provided an insight into the dual benefits of modulating the structure of nonwovens made of different deniers of fibre induced by optimised carding parameters for the enhancement of functional properties of needle-punched nonwovens.

2 Materials and Methods

Polyester fibre of three different deniers (3, 4 and 6 denier) and 64 mm length were used for the study. Box Behnken three factors three level design was used to optimisethe feeder, cylinder, and doffer speeds for improvement in the orientation of fibres in the carded web. The actual values of machine variables corresponding to coded levels are given in Table 1. A three factors three variable design generated is given in Table 2. Total 15 fabrics made of respective fibre denier were prepared on DILO nonwoven machine line having needle punching technique. The basis weight for all the fabrics was kept the same at 300 g/m^2 and fabrics were punched at 200 punches/cm^2 punch density and 10 mm needle penetration depth.

2.1 Measurement of Fibre Orientation in Carded Batt

Lindsley's technique and image analysis technique were used to measure the orientation of fibres in carded batt.

2.1.1 Lindsley's Technique

Lindsley's fibre combing and cutting method was widely used to study the orientation of fibres in sliver and roving[22] as well as in carded batt. In this method, the carded batt was clamped between the bottom plate and the top three plates of the device as shown in Fig. 1. The clamped carded batt was combed in a forward direction and fibres not clamped were discarded. The fibres protruding out of the forward plate after combing were cut at the edge of the forward plate. Then, the forward plate was removed and the portion under the forward plate was combed until the fibreswere fully straightened and parallel. The combed-out fibres were collected. The forward plate was then placed on its position and the projected portion of fibres from the edge of the forward plate after combing was cut through along the edge of the plate and then collected. Hence, it is apparent that the

Table 1 — Actual values of variables corresponding to coded levels

Variables	Coded levels		
	-1	0	1
Feeder speed (A), m/min	0.14	0.19	0.24
Cylinder speed (B), m/min	100	175	250
Doffer speed (D), m/min	4	6	8

Table 2 — Box Behnken design for carding machine variables

Sample No.	Feeder speed m/min	Cylinder speed m/min	Doffer speed m/min
1	0.24	175	8
2	0.24	175	4
3	0.14	250	6
4	0.19	250	8
5	0.19	175	6
6	0.14	175	8
7	0.19	100	4
8	0.24	100	6
9	0.24	250	6
10	0.14	100	6
11	0.19	250	4
12	0.19	175	6
13	0.19	175	6
14	0.19	100	8
15	0.14	175	4

Fig. 1 — Lindsley's instrument to measure fibre orientation

higher the curliness, hooks, and loops of fibres in the carded batt, the more will be the projected portion of fibres from the edge of the forward plate after combing.

Leont'eva coefficients, viz. proportion of curved fibre ends and coefficient of relative fibre parallelization, were used to measure the orientation of fibres[23]. The indices used for studying the fibre orientation in carded batt are described below:

$$\text{Proportion of curved fibre ends } (\rho) = \frac{E}{E+N} \quad \ldots (1)$$

$$\text{Coefficient of relative fibre parallelization } (K_\rho) = 1 - \frac{E}{C+E+N} \times 100 \quad \ldots (2)$$

The proportion of curved fibre ends (ρ) indicates curved fibre ends as well as their length in carded batt. Thus, the more the fibre curliness in carded batt, the more is the value of ρ.

The coefficient of relative fibre parallelization (K_ρ) represents the degree of fibre parallelization and straightening in carded batt. Thus, the more the fibre straightening and parallelization in carded batt, the more is the value of K_ρ.

In Eqs (1) and (2), *C* is the weight of combed out portion under the forward plate; *E*, the weight of the projected portion from the edge of the forward plate after combing; and *N*, the weight of material after combing and cutting under the forward plate.

2.1.2 Measurement ofAnisotropy of Inclination Angle of Fibres

In this method, the nonwoven fabrics were analysed by using an SMZ2500 Nikon microscope with NIS elements software. The fabrics were illuminated under the microscope at ×25 magnification. Using the NIS software, a certain portion of the sample was framed and several angles at different fibre inclinations were taken with respect to a baseline as shown in Fig. 2. Accordingly, the other portion of the sample was framed and the same procedure was repeated. In this way, 5000 readings for each sample were taken from various places across the sample. Finally, the frequency distribution of inclination angles was obtained. The histogram of fibre inclination was devised with the help of a mathematical model[17], as given below:

$$p(\psi) = \frac{1}{\pi} \frac{\eta}{\eta^2 - (\eta^2 - 1)cos^2(\psi)}$$

where p(ψ) is the probability density function of all obtained inclination angles; and η, the anisotropy.

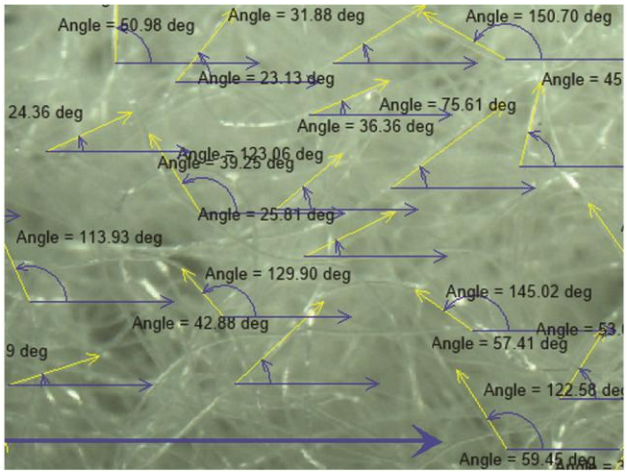

Fig. 2 — Measurement of fibre inclination angle using image processing technique on NIS software

The value of anisotropy (η) = p(0)/p(π/2), where p(0) means maximum probability density of fibre orientation and p(π/2) represents minimum probability density of fibre orientation.

2.1.3 Mean Flow Pore Size

The capillary flow porometer (POROLUX™1000, Germany) was used to measure the mean flow pore size of the nonwoven fabrics. The fabrics were wetted with a low surface tension liquid (POROFIL) and placed in a sealed chamber which was pressurised with nitrogen gas. An average of ten readings was taken.

3 Results and Discussion

The structural parameters measured for each fibre denier with respect to different sets of carding parameters as obtained from the Box- Behnken design are summarised in Table 3.

3.1 Fibre Orientation in Carded Batt

Fibre orientation was measured in terms of the proportion of curved fibre ends and the coefficient of relative fibre parallelisation by using Lindsley's technique, and the results are summarised in Table 3.

A- Proportion of curved fibre ends, B- Coefficient of relative fibre parallelisation, C- Anisotropy of inclination angle of fibres, D- Tortuosity factor using Vallabh's formula, and E- Tortuosity factor using proposed formula.

3.1.1 Proportion of Curved Fibre Ends in Carded Batt

The variance analysis of the proportion of curved fibre ends in carded batt made from all three considered deniers has been carried out. To avoid

Table 3 — Structural parameters for different fibre deniers with respect to designed sets of carding parameters

Sample No.	Carding parameters			3 Denier					4 Denier					6 Denier				
	Feeder speed m/min	Cylinder speed m/min	Doffer speed m/min	A	B	C	D	E	A	B	C	D	E	A	B	C	D	E
1	0.24	175	8	0.2850	0.5251	2.67	1.0963	1.0903	0.2570	0.5635	3.12	1.0650	1.0644	0.2122	0.5977	3.25	1.0475	1.0450
2	0.24	175	4	0.3875	0.4417	2.34	1.0896	1.0866	0.3526	0.4523	2.64	1.0617	1.0595	0.2897	0.5420	2.80	1.0431	1.0418
3	0.14	250	6	0.2337	0.5836	3.15	1.1101	1.0972	0.2238	0.5903	3.35	1.0712	1.0718	0.1744	0.6683	3.58	1.0529	1.0510
4	0.19	250	8	0.2470	0.5563	2.83	1.1025	1.0921	0.2247	0.5764	3.42	1.0745	1.0686	0.1826	0.6612	3.60	1.0532	1.0512
5	0.19	175	6	0.2448	0.5733	2.93	1.1083	1.0940	0.2127	0.6153	3.33	1.0698	1.0770	0.2317	0.5919	3.53	1.0524	1.0472
6	0.14	175	8	0.2824	0.5367	2.71	1.1006	1.0915	0.2594	0.5495	3.38	1.0731	1.0720	0.1739	0.6692	3.62	1.0554	1.0511
7	0.19	100	4	0.3952	0.4322	2.19	1.0865	1.0838	0.3532	0.4472	2.68	1.063	1.0629	0.2891	0.545	2.97	1.0432	1.0421
8	0.24	100	6	0.3718	0.4436	2.37	1.0913	1.0887	0.3384	0.4596	2.56	1.0581	1.0574	0.2949	0.4973	2.71	1.04	1.0414
9	0.24	250	6	0.2844	0.5275	2.69	1.0969	1.0904	0.2560	0.5662	3.04	1.0646	1.0638	0.2127	0.5968	3.25	1.0462	1.0455
10	0.14	100	6	0.3524	0.4637	2.45	1.0931	1.0894	0.3207	0.4748	2.85	1.0632	1.0635	0.2629	0.5754	3.14	1.0452	1.0441
11	0.19	250	4	0.3105	0.5125	2.6	1.0946	1.0896	0.2825	0.5284	3.14	1.0655	1.0649	0.2099	0.6107	3.32	1.0482	1.0456
12	0.19	175	6	0.2459	0.5716	2.85	1.1035	1.0922	0.2227	0.5923	3.25	1.0682	1.0674	0.1843	0.6114	3.42	1.0514	1.0468
13	0.19	175	6	0.2380	0.5734	2.89	1.1066	1.0924	0.2166	0.6153	3.16	1.0659	1.0660	0.2107	0.6085	3.39	1.0487	1.0463
14	0.19	100	8	0.3882	0.4361	2.26	1.089	1.0849	0.3596	0.4465	2.75	1.0611	1.0633	0.2774	0.5696	3.1	1.0448	1.0436
15	0.14	175	4	0.2813	0.5395	2.79	1.1024	1.0918	0.2588	0.5557	3.18	1.0669	1.0667	0.1835	0.6244	3.4	1.0502	1.0468

A-Proportion of curved fibre ends, B- Coefficient of relative fibre parallelistion, C- Anisotropy, D- Tortuosity factor using Vallabh's formula, and E- Tortuosity factor using proposed formula

Table 4 — Variance analysis of proportion of curved fibre ends in carded batt for 3 denier fibres

Source	Sum of squares	Df	Mean square	F-value	p-value	
Model	0.0501	9	0.0056	71.21	< 0.0001	Significant
A-Feeder speed	0.0040	1	0.0040	51.18	0.0008	
B-Cylinder speed	0.0233	1	0.0233	298.39	< 0.0001	
C-Doffer speed	0.0037	1	0.0037	47.26	0.0010	
AC	0.0027	1	0.0027	34.25	0.0021	
BC	0.0008	1	0.0008	10.20	0.0242	
A^2	0.0016	1	0.0016	20.34	0.0063	
B^2	0.0081	1	0.0081	103.93	0.0002	
C^2	0.0076	1	0.0076	97.32	0.0002	
Residual	0.0004	5	0.0001			
Lack of Fit	0.0004	3	0.0001	6.56	0.1351	Not significant
Pure Error	0.0000	2	0.0000			
Cor Total	0.0505	14				

repetition, the variance analysis of the proportion of curved fibre ends in carded batt made from 3 denier fibre is only reported and is shown in Table 4. The obtained quadratic model is found to be significant.

The response surface equations for the proportion of curved fibre ends for nonwoven fabrics made of 3, 4 and 6 denier fibres are represented in following equations having R^2 values of 0.939, 0.957 and 0.974 respectively:

3 Denier

Proportion of curved fibre ends in carded batt = $0.243+ 0.022 \times A - 0.054\times B - 0.022 \times C + 0.008 \times AB - 0.026 \times AC - 0.014 \times BC + 0.021\times A^2 + 0.047\times B^2 + 0.045\times C^2$ …(3)

4 Denier

Proportion of curved fibre ends in carded batt = $0.217 + 0.018 \times A - 0.048 \times B - 0.018 \times C + 0.004 \times AB - 0.024 \times AC - 0.016 \times BC + 0.022 \times A^2 + 0.045 \times B^2 + 0.042 \times C^2$ … (4)

6 Denier

Proportion of curved fibre ends in carded batt = $0.171 + 0.014 \times A - 0.012 \times B - 0.008 \times C + 0.002 \times AC - 0.0002\times BC + 0.016\times A^2 + 0.015 \times B^2 + 0.007 \times C^2$ …(5)

The obtained R^2 values represent a strong correlation between the proportion of curved fibre ends and the carding parameters. These equations are used to draw the 3D surface plots of the considered carding parameters in relation to the proportion of curved fibre ends.

Figures 3 (a) - (c) show the 3D surface plots of cylinder speed *vs* doffer speed at constant feeder speed in relation to the proportion of curved fibre ends in carded batt made of 3 denier, 4 denier and 6 denier fibres respectively. It is observed that with an increase in cylinder speed, the proportion of curved fibre ends decrease and then increase. The proportion of curved fibre ends shows a decrease followed by an increase with increase in doffer speed. Similar trends are also

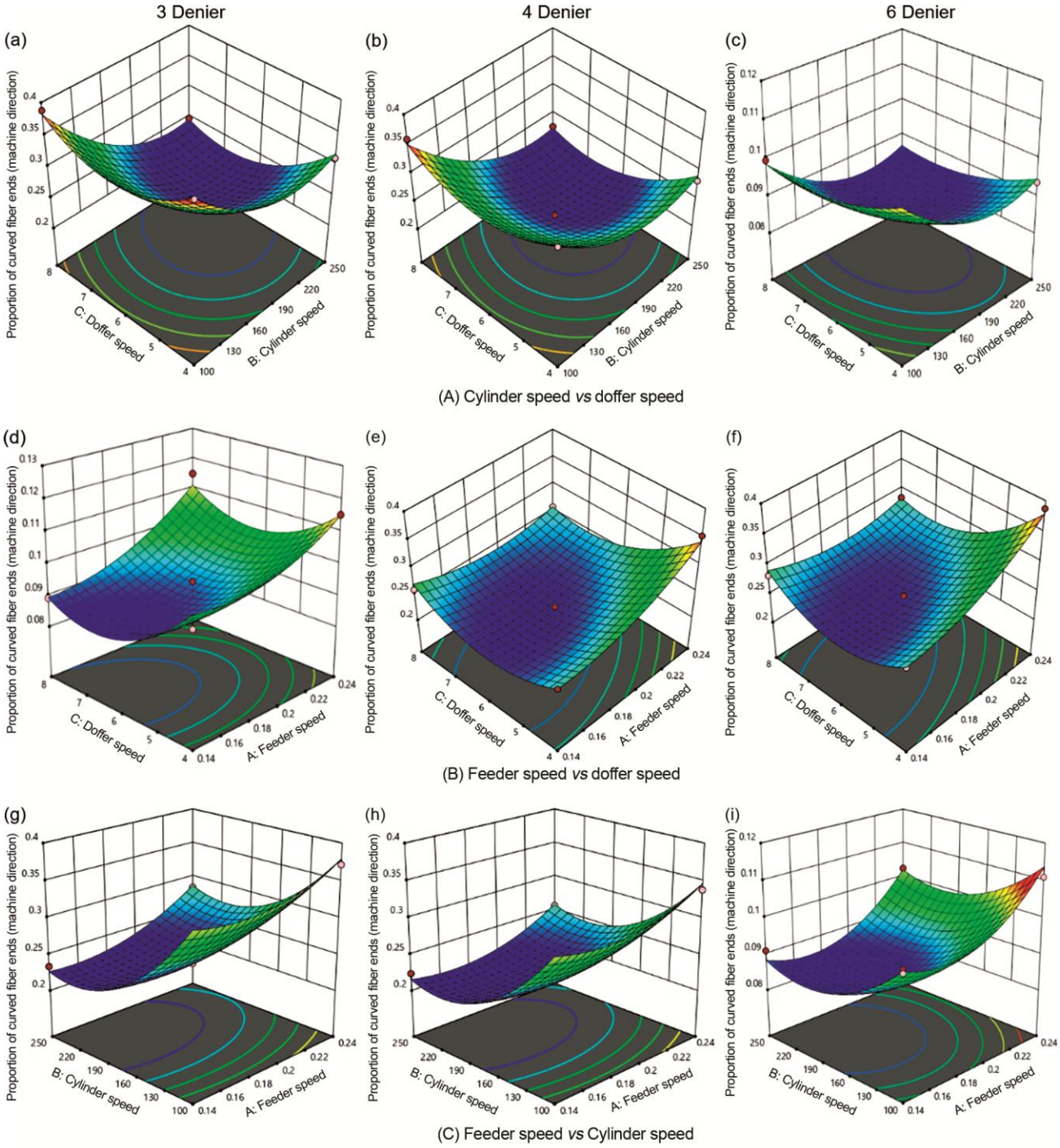

Fig. 3 — Proportion of curved fibre ends in carded batt made from different denier fibres (A) - cylinder speed *vs* doffer speed (0.19 m/min feeder speed), (B) – feeder speed *vs* doffer speed (175 m/min cylinder speed), and (C) feeder speed *vs* cylinder speed (6 m/min doffer speed)

obtained for all three deniers of fibre. The obtained trends are justified based on the force which acts on the fibres in various directions, depending on their position in the fibrousassembly during the carding process. Fibre denier plays an important role in governing the degree of opening of the fibre mass.

The more the fibre denier, the less is the frictional resistance offered to the opening process, which results in improved fibre opening. Increased cylinder speed increases the centrifugal force acting on the fibres, which causes better fibre opening and individualisation. Thus, the fibres get more

straightened and parallel in the carded web. These factors contribute towards better orientation of the fibres in the carded web and, accordingly, reduce the value of the proportion of curved fibre ends, but towards higher cylinder speed, the fibres are subjected to very high forces and get haphazardly transferred to the doffer which increases the proportion of curved fibre ends. With increased doffer speed, the trailing hooks of fibres get removed while the cylinder contributes to the removal of the leading and both end hooks and thus results inimproved fibre orientation in the carded web. However, towards higher doffer speed, the fibre transfer efficiency from cylinder to doffer is adversely affected due to the change in speed ratio which causes an increase in the proportion of curved fibre ends.The proportion of curved fibre ends shows a decrease and then increase with the increase in both cylinder and doffer speeds at different feeder speeds, but the proportion of curved fibre ends increases with increase in feeder speed because at constant feeder speed, both cylinder and doffer speeds contribute positively towards the removal of hooks and lead to fibre straightening. Hence, this decreases the value of proportion of curved fibre ends. However, further increasein speed hampers the fibre transfer from cylinder to doffer, which causes an increase in the proportion of curved fibre ends.

The results show an increase in the proportion of curved fibre ends with increase in feeder speed. It is known that with increased feeder speed, the thickness of the feed material to taker-in increases. Therefore, the height of the wire points of the taker-in is not effective for the entire thickness of the feed material. The bottommost layers of the feed material do not get a chance to get open properly. Moreover, an increase in feeder speed increases cylinder loading, which hampers fibre transfer efficiency from cylinder to doffer. Thus, an increase in feeder speed induces disorientation in the fibres which is responsible for increasing the proportion of curved fibre ends. It should also be noted that higher stresses are induced in finer fibres as compared to coarser fibres which also contributes towards the latter's increase in proportion of curved fibre ends. The proportion of curved fibre ends follows a decreasing trend with an increase in denier of fibres. This is due to insufficient opening and individualisation of finer fibres as compared to coarser fibres. The coarser fibres have higher bending rigidity, so they are less prone to distortions and can be easily straightened out.

Figures 3 (d) - (f) show the 3D surface plots of feeder speed *vs* doffer speed at constant cylinder speed in relation to proportion of curved fibre ends in carded batt made from 3 denier, 4 denier and 6 denier fibres respectively. It is observed that carded batts made from 3 denier fibres depict an increase in the proportion of curved fibre ends with the increase in feeder speed. The obtained trend is found to be applicable for carded batts made from other denier fibres also. With increased feeder speed, there is less penetration of wire points through the increased thickness of feed material to taker-in, which hampers the fibre opening process and increases load on the cylinder. Moreover, the transfer efficiency of cylinder gets adversely affected. Thus, the formation of hooks increases with increase in feeder speed. Slight reduction in proportion of curved fibre ends is due to disorientation caused by increased feeder speed which is taken care of by the cylinder speed. However, as the feeder speed progresses, this compensatory effect reduces. With increased doffer speed, the proportion of curved fibre ends reduces and then slightly increases. The reduction is due to positive influence of cylinder and doffer speeds in reduction of hooks and fibre straightening. The increase in number of fibre hooks towards higher doffer speed leads to an increase in proportion of curved fibre ends. The proportion of curved fibre ends follow a decrease and then increase with the increase in both feeder and doffer speed increase. This is attributed to increase in number of hooks caused by increased feeder speed which gets compensated by cylinder and doffer speeds. However, on further increasing the speeds, the fibres get disoriented and lead to an increase in curved fibre ends. It is noted that with an increase in fibre denier, the proportion of curved fibre ends reduces due to the same reasons as explained above.

Figures 3 (g) - (i) show the 3D surface plots of feeder speed *vs*cylinder speed at constant doffer speed in relation to the proportion of curved fibre ends in carded batt made from 3 denier, 4 denier and 6 denier fibres respectively. The carded batt made from 3 denier fibres first shows a slight reduction in the proportion of curved fibre ends and then shows a continuous increase with increased feeder speed. The proportion of curved fibre ends follows a reduction with an increase in cylinder speed but a slight increase can be observed towards higher cylinder speed. This trend is true for carded batts made from 4 and 6 denier fibres. The results depict a decrease and then an increase in the proportion of curved fibre ends with

the increase in both feeder and cylinder speeds. Initially, with an increase in feeder speed, the hooks so formed are straightened out by an increase in cylinder speed but the fibres get disoriented towards higher speeds.

3.1.2 Coefficient of Relative Fibre Parallelisation

Table 5 represents the variance analysis of the coefficient of relative fibre parallelisation in carded batt made of 3 denier fibres.The obtained quadratic model is found to be significant. Variance analysis of 3 denier fibre is only represented to avoid the repetition.

The response surface equations for the coefficient of relative fibre parallelisation in carded batt made of 3, 4 and 6 denier fibres are shown in following equations having R^2 values of 0.954, 0.982 and 0.960 respectively:

3 Denier

Coefficient of relative fibre parallelisation in carded batt = $0.573 - 0.023 \times A + 0.050 \times B + 0.016 \times C - 0.009 \times AB + 0.021 \times AC + 0.010 \times BC - 0.020 \times A^2 - 0.047 \times B^2 - 0.041 \times C^2$ …(6)

4 Denier

Coefficient of relative fibre parallelisation in carded batt = $0.607 - 0.016 \times A + 0.054 \times B + 0.019 \times C - 0.002 \times AB + 0.029 \times AC + 0.012 \times BC - 0.027 \times A^2 - 0.058 \times B^2 - 0.050 \times C^2$ ...(7)

6 Denier

Coefficient of relative fibre parallelisation in carded batt = $0.604 - 0.037 \times A + 0.044 \times B + 0.022 \times C + 0.003 \times AB + 0.004 \times AC + 0.008 \times BC - 0.006 \times A^2 - 0.015 \times B^2 + 0.009 \times C^2$ …(8)

These equations are used to draw the 3D surface plots of considered carding parameters in relation to the coefficient of relative fibre parallelisation.

Figure 4 (a) - (c) show the 3D surface plots of cylinder speed *vs* doffer speed at different feeder speeds in relation to coefficient of relative fibre parallelisation in carded batt made from 3 denier, 4 denier and 6 denier fibres respectively. The results of carded batts made from 3 denier fibres record an increase in coefficient of relative fibre parallelisation with increase in cylinder speed, but with a slight decrease towards higher cylinder speed. It is attributed to the straightening of fibre imparted by cylinder speed, as already discussed above in the case of the proportion of curved fibre ends. However, at higher cylinder speed, extra force acts on the fibres which hampers the fibre straightening and transfer efficiency of the cylinder to the doffer. The results depict an initial increase and then a decrease in the coefficient of relative fibre parallelisation with the increase in doffer speed.

However, increased cylinder and doffer speeds shows an increase in the coefficient of relative fibre parallelisation with a slight decrease towards higher speeds.As discussed above, the combined effect of both the cylinder and doffer helps in the removal of hooks and makes fibre straight, whereas towards higher doffer speed, the chances of hook formation increase. The obtained trends are applicable for 4 denier fibres as well. However, carded batt made from 6 denier fibres shows an increase in the coefficient of relative fibre parallelisation with the increase in cylinder speed. The increase in both cylinder and doffer speeds also increases the coefficient of relative fibre parallelisation. The results reveal an increase in the coefficient of relative fibre parallelisation with increased fibre denier. The reasoning of above trends is the same as discussed in the case of proportion of curved fibre ends.

Figures 4 (d) - (f) show the 3D surface plots of feeder speed *vs* doffer speed at different cylinder

Table 5 — Variance analysis of the coefficient of relative fibre parallelisation in carded batt made of 3 denier fibres

Source	Sum of squares	Df	Mean square	F-value	p-value	
Model	0.0402	9	0.0045	45.96	0.0003	Significant
A-Feeder speed	0.0043	1	0.0043	44.29	0.0012	
B-Cylinder speed	0.0204	1	0.0204	210.20	< 0.0001	
C-Doffer speed	0.0021	1	0.0021	21.12	0.0059	
AC	0.0019	1	0.0019	19.10	0.0072	
A^2	0.0009	1	0.0009	9.16	0.0292	
B^2	0.0065	1	0.0065	67.00	0.0004	
C^2	0.0047	1	0.0047	48.84	0.0009	
Residual	0.0005	5	0.0001			
Lack of Fit	0.0003	3	0.0001	0.8614	0.5767	Not significant
Pure Error	0.0002	2	0.0001			
Cor Total	0.0407	14				

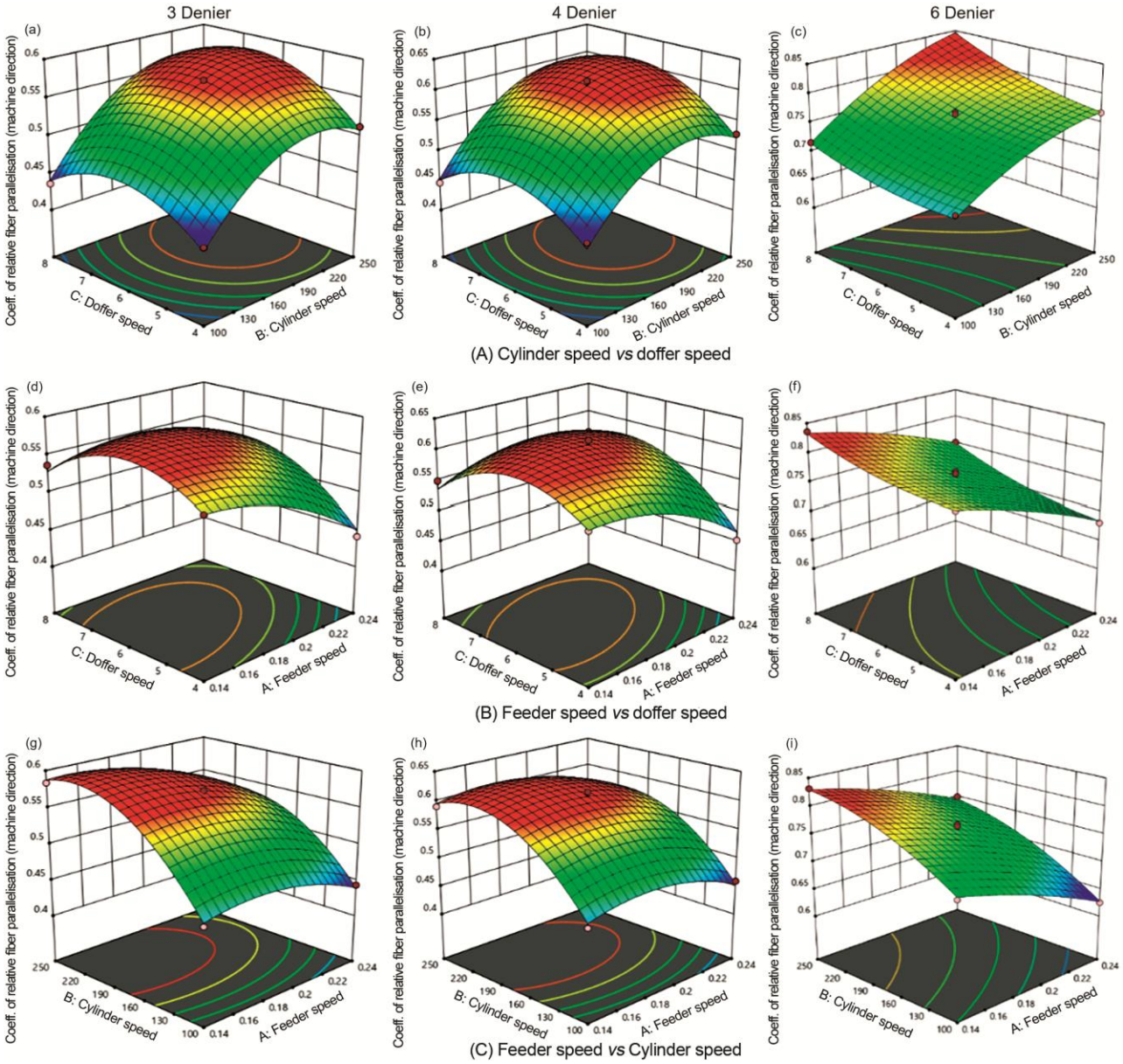

Fig. 4 — Coefficient of relative fibre parallelisation in carded batt made from different denier fibres (A) - cylinder speed *vs* doffer speed (0.19 m/min feeder speed), (B) – feeder speed *vs* doffer speed (175 m/min cylinder speed) and (C) feeder speed *vs* cylinder speed (6 m/min doffer speed)

speeds in relation to coefficient of relative fibre parallelisation in carded batt made from 3 denier, 4 denier and 6 denier fibres respectively. The results of carded batts made from 3 denier fibres show a reduction in the coefficient of fibre parallelisation with the increase in feeder speed. The reasons for poor orientation of fibres caused by increased feeder speed are already discussed in the case of the proportion of curved fibre ends. The coefficient of relative fibre parallelisation increases and then decreases with increased doffer speed. This trend is true for carded batts made from 4 denier fibre also. As discussed in section **3.1.1**, the positive impact of both cylinder and doffer helps in the removal of hooks and fibre straightening, whereas a further increase in doffer speed at constant cylinder speed reduces the fibre transfer efficiency.

However, carded batts made from 6 denier fibres increases the coefficient of relative fibre parallelisation with increase in doffer speed. The coefficient of relative fibre parallelisation reveals an increase and then decrease with the increase in both feeder and doffer speeds. This is because formation of leading hooks due to feeder and doffer speeds is taken

care of by the cylinder speed. Hence, the fibres get more parallel. Further increase of speed at constant cylinder speed creates disorientation in carded web and thus reduces coefficient of relative fibre parallelisation. The results reveal an increase in the coefficient of relative fibre parallelisation with increased fibre denier.

Figures 4 (g) -(i) show the 3D surface plots of feeder speed *vs* cylinder speed at different doffer speeds in relation to the coefficient of relative fibre parallelisation in carded batt made from 3 denier, 4 denier and 6 denier fibres, respectively. The results show a reduction in the value of coefficient of relative fibre parallelisation with increase in feeder speed. However, increase in cylinder speed initially increases the coefficient of relative fibre parallelisation, but a slight drop is noticed towards higher cylinder speed. This trend is true for all fibre deniers, except 6 denier fibres where the coefficient of relative fibre parallelisation increases continuously with increase in cylinder speed. This is due to the improved straightening of fibres imparted by cylinder speed. The disorientation caused by increased feeder speed leads to reduction in coefficient of relative fibre parallelisation. However, the coefficient of relative fibre parallelisation increases and then decreases with the increase in both feeder and cylinder speeds because initial disorientation caused by feeder speed is taken care of by the cylinder and doffer speeds but towards higher feeder and cylinder speeds, the fibre transfer efficiency is adversely affected, and causes fibredisorientation. The results confirmed an increase in coefficient of relative fibre parallelisation with increased fibre denier and the reasons which hold true for the proportion of curved fibre ends are also valid here.

3.2 Anisotropy of Inclination Angle of Fibres

The effect of carding parameters on anisotropy of inclination angle of fibres of nonwoven fabric made of different denier fibres is summarised in Table 3.

To avoid repetition, the variance analysis of the anisotropy of inclination angle of fibres of nonwoven made from 3 denier fibres is reported and is shown in Table 6. The obtained quadratic model is found to be significant.

The response surface equations for anisotropy of inclination angle of fibres in terms of coded factors and significant model terms for each fibre denier are represented below having R^2 values of 0.936, 0.969 and 0.951 respectively:

3 Denier

Anisotropy of inclination angle of fibres = $2.89 - 0.129 \times A + 0.250 \times B + 0.069 \times C - 0.095 \times AB + 0.102 \times AC + 0.040 \times BC - 0.034 \times A^2 - 0.191 \times B^2 - 0.229 \times C^2$ …(9)

4 Denier

Anisotropy of inclination angle of fibres = $3.247 - 0.174 \times A + 0.264 \times B + 0.130 \times C - 0.005 \times AB + 0.067 \times AC + 0.052 \times BC - 0.108 \times A^2 - 0.188 \times B^2 - 0.061 \times C^2$ …(10)

6 Denier

Anisotropy of inclination angle of fibres = $3.447 - 0.214 \times A + 0.231 \times B + 0.135 \times C + 0.025 \times AB + 0.062 \times AC + 0.042 \times BC - 0.134 \times A^2 - 0.144 \times B^2 - 0.051 \times C^2$ …(11)

The 3D surface plots of considered carding parameters in relation to the anisotropy of inclination angle of fibres are drawn using these equations.

Figures 5 (a) - (c) show the 3D surface plots of cylinder speed vs doffer speed at constant feeder speed in relation to anisotropy of inclination angle of

Table 6 — Variance analysis of anisotropy of inclination angle of fibres of nonwoven fabric made of 3 denier fibre

Source	Sum of squares	Df	Mean square	F-value	p-value	
Model	1.06	9	0.1179	181.92	< 0.0001	Significant
A-Feeder speed	0.1292	1	0.1292	199.35	< 0.0001	
B-Cylinder speed	0.5015	1	0.5015	773.94	< 0.0001	
C-Doffer speed	0.0388	1	0.0388	59.83	0.0006	
AB	0.0368	1	0.0368	56.78	0.0007	
AC	0.0419	1	0.0419	64.63	0.0005	
BC	0.0064	1	0.0064	9.93	0.0254	
B^2	0.1352	1	0.1352	208.65	< 0.0001	
C^2	0.1942	1	0.1942	299.78	< 0.0001	
Residual	0.0032	5	0.0006			
Lack of Fit	0.0005	3	0.0002	0.1352	0.9308	Not significant
Pure Error	0.0027	2	0.0013			
Cor Total	1.06	14				

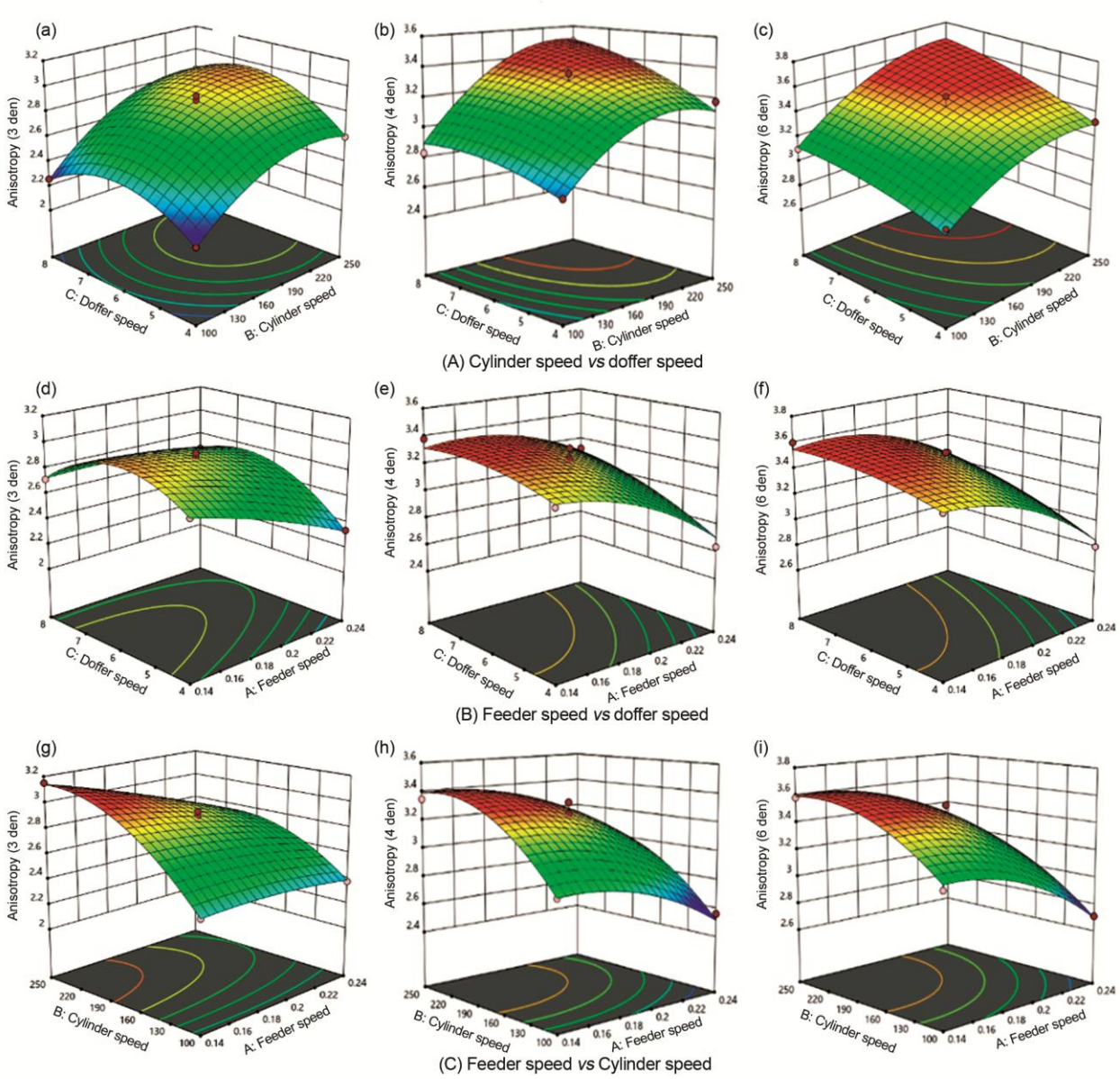

Fig. 5 — Anisotropy of inclination angle of fibres of nonwoven fabricmade from different denier fibres (A) - cylinder speed *vs* doffer speed (0.19 m/min feeder speed), (B) – feeder speed *vs* doffer speed (175 m/min cylinder speed), and (C) feeder speed *vs* cylinder speed (6 m/min doffer speed)

fibres of fabric made from fibre of different deniers. The 3D surface plots representing the anisotropy of inclination angle of fibres of nonwoven fabrics made from 3 denier fibres reveal that the anisotropy of inclination angle of fibres shows an increase with the increase in cylinder speed but a slight decrease towards higher cylinder speed. Anisotropy of inclination angle of fibres shows an initial increase and then a decrease with the increased doffer speed. Similar trends are also observed with nonwoven fabrics made from 4 denier and 6 denier fibres. Increased cylinder speed causes better fibre opening and individualisation and contributes towards improved fibre extent in carded web, thus reducing the fibre inclination angle. However, the fibres get haphazardly transferred towards doffer with higher cylinder speed, which reduces the anisotropy of inclination angle of fibres.

The anisotropy of inclination angle of fibres follows an increase and then decrease with the increase in both cylinder as well as doffer speeds at different feeder speeds, but the increase in feeder speed reduces

anisotropy of inclination angle of fibres because both cylinder and doffer speed contribute positively towards the removal of hooks at constant feeder speed. This leads to fibre straightening and thereby increases the anisotropy of inclination angle of fibres. However, further increase in speeds hampers fibre transfer from cylinder to doffer which causes a reduction in anisotropy of inclination angle of fibres. The results record a reduction in anisotropy of inclination angle of fibres with the increase in feeder speed. The increased feeder speed causes an increase in thickness of feed material which provides lesser opportunity to wire point of taker-in to open the bottommost layers. Moreover, increase in the feeder speed increases cylinder loading which hampers fibre transfer efficiency from cylinder to doffer. Anisotropy of inclination angle of fibres follows an increasing trend with increase in fibre denier. The obtained trend is due to insufficient opening and individualisation offiner fibres as compared to coarser fibres. As discussed above, the higher value of the proportion of curved fibre ends along with the lower value of the coefficient of relative fibre parallelisation in the case of finer fibres imparts low anisotropy of inclination angle of fibres.

Figures 5 (d) - (f) show the 3D surface plots of feeder speed *vs* doffer speed at constant cylinder speeds in relation to the anisotropy of inclination angle of fibres of nonwoven fabric made from 3 denier, 4 denier, and 6 denier fibres respectively. The anisotropy of inclination angle of fibres made of 3 denier fabrics shows a decrease with increase in feeder speed. As discussed above, the increased feeder speed induces disorientation of fibres in the carded web which is responsible for the reduction in the anisotropy of inclination angle of fibres. Increased doffer speed initially increases the anisotropy of inclination angle of fibresbecause the combined effect of doffer and cylinder speeds helps in the removal of hooks, thus improving the fibre straightening. However, towards higher doffer speed, the fibre transfer efficiency gets disturbed, which increases the chances for hook formation. The fabrics made from 4 and 6 denier fibres show a decrease followed by an increase in the value of anisotropy of inclination angle of fibres with increase in doffer speed. However, an increase in both feeder and doffer speeds follow an increase and then a decrease in anisotropy of inclination angle of fibres at respective cylinder speeds, but the increased cylinder speed registers an increase in the value of anisotropy of inclination angle of fibres. The increase in feeder, cylinder and doffer speeds noticed an increase and then decrease in anisotropy of inclination angle of fibres. The positive contributions of cylinder and doffer speeds and negative contribution of feeder speed on anisotropy of inclination angle of fibres support the obtained trends. Further, an increase in the anisotropy of inclination angle of fibres is noticed with increased fibre deniers.

Figures 5 (g) - (i) show the 3D surface plots of feeder speed *vs* cylinder speed at constant doffer speed in relation to anisotropy of inclination angle of fibres of nonwoven fabric made from different denier fibres. It is observed from the 3D surface plots that anisotropy of inclination angle of fibres of fabrics made from 3 denier fibres shows a decrease with increase in feeder speed, but an increase with increased cylinder speed at constant doffer speed. Similar trends are observed in nonwoven fabrics made from other considered deniers. The contribution of feeder and cylinder speeds towards fibre orientation in the carded web has already been discussed above. However, increase in both feeder and cylinder speeds follow an increasing and then decreasing trends of anisotropy of inclination angle of fibre at respective doffer speed, but further increase in doffer speed observes an increase and then decrease in anisotropy. This is because, disorientation caused by increased feeder speed gets compensated by cylinder and doffer speeds. However, further increase in feeder speed along with cylinder speed at constant doffer speed hampers the speed ratio required for efficient fibre transfer, thus increasing the chances of hook formation in carded web. In this case also, the anisotropy of inclination angle of fibres value was found to increase with increased fibre denier.

Overall, it can be concluded that the results of the proportion of curved fibre ends and the coefficient of relative fibre parallelisation, support the trends of anisotropy of inclination angle of fibres.

3.3 Tortuosity Factor

Vallabh *et al.*[24-26] have established a relationship between the tortuosity factor and fibre diameter, porosity, and number of layers in the web geometry for calculating the tortuosity factor using CFD simulations. The formula proposed by them is used to calculate the tortuosity factor and results are illustrated in Table 3. Results reveal that the tortuosity factor is highly influenced by the measured proportion of curved fibre ends, the coefficient of relative fibre parallelisation and anisotropy of inclination angle of

fibre. Therefore, it is realized that tortuosity factor can also serve as an important factor to gauge the structure of the nonwoven influenced by orientation of fibres in carded web. Accordingly, nonlinear regression technique is used to establish a relationship between the tortuosity factor and the measured structural and physical characteristics, viz. fibre diameter, proportion of curved fibre ends, coefficient of relative fibre parallelisation, anisotropy of inclination angle of fibres, and mean flow pore size of the nonwoven fabrics. Following equation has been derived to establish the tortuosity factor as a function of measured structural and physical parameters, having R^2 value of 0.94:

$$\text{Tortuosity factor} = 2.6007 - 0.02211 \times X_1 - 4.2533 \times X_2 - 2.539 \times X_3 - 0.1448 \times X_4 - 0.0146 \times X_5 + 0.07470 \times X_1 \times X_2 + 0.0630 \times X_1 \times X_3 - 0.0125 \times X_1 \times X_4 - 0.0011 \times X_1 \times X_5 + 4.8189 \times X_2 \times X_3 - 0.2160 \times X_2 \times X_4 - 0.0474 \times X_2 \times X_5 + 0.0614 \times X_3 \times X_4 - 0.0402 \times X_3 \times X_5 + 0.0078 \times X_4 \times X_5 + 0.0008 \times {X_1}^2 + 3.5885 \times {X_2}^2 + 0.7756 \times {X_3}^2 + 0.0381 \times {X_4}^2 + 0.0004 \times {X_5}^2 \quad \ldots(12)$$

where X_1 is the fibre diameter; X_2, the proportion of curved fibre ends; X_3, the coefficient of relative fibre parallelisation; X_4, the anisotropy of inclination angle of fibre; and X_5, the mean flow pore size.

It is depicted from above equation that fibre diameter and mean flow pore size have a dominating influence on the tortuosity factor followed by proportion of curved fibre ends, coefficient of relative fibre parallelisation and anisotropy of inclination angle of fibre. The values of tortuosity factor obtained from Vallabh's formula and proposed formula reveal a very good resemblance, but the values obtained from the proposed formula are found slightly lower as compared to Vallabh's formula. The obtained trends are applicable to all the considered fibre deniers. However, the tortuosity factor notices a reduction with increased denier of fibre.

To realize the importance of orientation of fibres, the measured values for best and worst orientation of fibresfor respective fibre denier in carded batts and their corresponding characteristics obtained by optimising the carding parameters, are given in Table 3. It is evident from Tables 3 and 7 that how different combinations of carding parameters are significantly influencing measured structural characteristics of nonwoven fabrics.

Table 7 shows that fabric 3 made of 3 denier fibre provides lower value of proportion of curved fibre ends but higher values of coefficient of relative fibre parallelisation and anisotropy of inclination angle of fibre as compared to fabric 7 which is also made of 3 denier fibres. Therefore, it is inferred that fabric 3 possesses better orientation of fibres as compared to fabric 7. Further, it is also observed that value of mean flow pore size of fabric 3 is found to be lower than that of fabric 7. Hence, results confirm that mean flow pore size is governed by orientation of fibres in carded web because improved fibre orientation provides closeness of fibre as discussed above, which results in a decrease in mean flow pore size. Accordingly, the results also provide higher value of tortuosity factor for fabric 3 as compared to fabric 7. Therefore, it is apparent that the improved orientation of fibres which brings the fibre closer in carded web influence by carding parameters is responsible for higher value of tortuosity factor. The same trends hold

Table 7 — Tortuosity factor influenced by physical and structural parameters

Sample No.	Feeder speed m/min	Cylinder speed m/min	Doffer speed m/min	Fibre denier	Fibre diameter µm	Proportion of curved fibre ends	Coefficient of relative fibre parallelisation	Anisotropy of inclination angle of fibre	Mean flow pore size µm	Tortuosity factor	
										Vallabh's formula	Proposed formula
3	0.14	250	6	3.0	17.4	0.2337	0.5836	3.15	21.12	1.1101	1.0972
7	0.19	100	4	3.0	17.4	0.3952	0.4322	2.19	27.50	1.0865	1.0838
5	0.19	175	6	4.0	20.2	0.2127	0.6153	3.33	25.32	1.0698	1.0770
14	0.19	100	8	4.0	20.2	0.3596	0.4465	2.75	29.51	1.0611	1.0633
6	0.14	175	8	6.0	25.6	0.1739	0.6692	3.62	35.03	1.0554	1.0511
8	0.24	100	6	6.0	25.6	0.2949	0.4973	2.71	45.93	1.040	1.0414

Table 8 — Variance analysis of tortuosity factor in nonwoven fabric made of 3 denier fibre

Source	Sum of squares	Df	Mean square	F-value	p-value	
Model	0.0006	9	0.0001	13.29	0.0054	Significant
A-Feeder speed	0.0001	1	0.0001	20.38	0.0063	
B-Cylinder speed	0.0002	1	0.0002	42.14	0.0013	
C-Doffer speed	0.0000	1	0.0000	6.25	0.0445	
B^2	0.0001	1	0.0001	24.92	0.0041	
C^2	0.0001	1	0.0001	20.75	0.0061	
Residual	0.0000	5	4.617E-06			
Lack of Fit	0.0000	3	3.512E-06	0.5599	0.6916	Not significant
Pure Error	0.0000	2	6.274E-06			
Cor Total	0.0006	14				

true for other two considered deniers of fibre. However, tortuosity factor notices a reduction with increased denier of fibre. Therefore, proposed Eq. (13) confirmsthat fibre orientation in carded web influenced by denier specific carding parameters plays a significant role in determining the tortuosity of nonwoven fabrics.

Table 8 represents the variance analysis of tortuosity factor in nonwoven fabric made from 3 denier fibres. The obtained quadratic model is observed to be significant.

Following equations represent the response surface equations of tortuosity factor for 3, 4 and 6 denier fibres having R^2 values 0.969, 0.959 and 0.964 respectively:

3 Denier

$$\text{Tortuosity factor in fabric} = 1.096 - 0.003 \times A + 0.005 \times B + 0.002 \times C - 0.002 \times AB + 0.002 \times AC + 0.001 \times BC - 0.002 \times A^2 - 0.006 \times B^2 - 0.005 \times C^2 \quad \ldots(13)$$

4 Denier

$$\text{Tortuosity factor in fabric} = 1.068 - 0.003 \times A + 0.004 \times B + 0.002 \times C - 0.001 \times AB - 0.001 \times AC + 0.003 \times BC - 0.002 \times A^2 - 0.002 \times B^2 \quad \ldots(14)$$

6 Denier

$$\text{Tortuosity factor in fabric} = 1.048 - 0.003 \times A + 0.003 \times B + 0.002 \times C + 0.001 \times BC \quad \ldots(15)$$

These equations were used to draw the 3D surface plots of considered carding parameters in relation to tortuosity factor in nonwoven fabric.

Figures 6(a) - (c) show the 3D surface plots of cylinder speed *vs* doffer speed at constant feeder speed in relation to tortuosity factor in nonwoven fabric made from fibre of different deniers. The 3D surface plots depict an increase in tortuosity factor with increase in cylinder speed, followed by a decrease towards higher cylinder speeds.

The tortuosity factor follows an increase and then slight decrease towards higher doffer speed. Similar trends are also observed for nonwoven fabrics made from 4 denier and 6 denier fibres. An increase in cylinder speed exerts an increasing centrifugal force on the fibres, which results in better fibre opening and parallelisation. The fibres are better oriented with a lower value of proportion of curved fibre ends and higher values of coefficient of relative fibre parallelisation and anisotropy of inclination angle of fibres. Accordingly, the fibres remain close to each other, resulting in a compact structure that is responsible for the higher tortuosity factor. However, as cylinder speeds increase, fibres become haphazardly arranged and randomly oriented. This results in a more porous structure having a larger mean flow pore size and thus possesses a lower tortuosity factor. The increased doffer speed initially improves the fibre straightening, but a further increase in doffer speed adversely affects the efficiency of fibre transfer, thus influencing the tortuosity factor accordingly. It is depicted that with increase in both cylinder speed and doffer speed, the tortuosity factor improves. However, towards higher cylinder and doffer speeds the changes in speed ratios influence the effectiveness of fibre transfer which induces less tortuosity in the fibrous assembly. The results register a decline in the value of tortuosity factor with the increase in denier of the fibres. This is because, higher diameter and bending rigidity of coarser denier fibres do not get closely packed in the fibrous assembly.

Figures 6 (d) - (f) show the 3D surface plots of feeder speed *vs* doffer speed at constant cylinder speed in relation to tortuosity factor in nonwoven fabric made from fibre of different deniers. The results of 3D surface plots observe an initial increase and then a decrease in tortuosity factor with increased feeder speed. The increase in tortuosity value is due to better straightening and parallelisation of the fibres. However, towards higher feeder speed, disorientation is induced in the fibrous assembly which results in

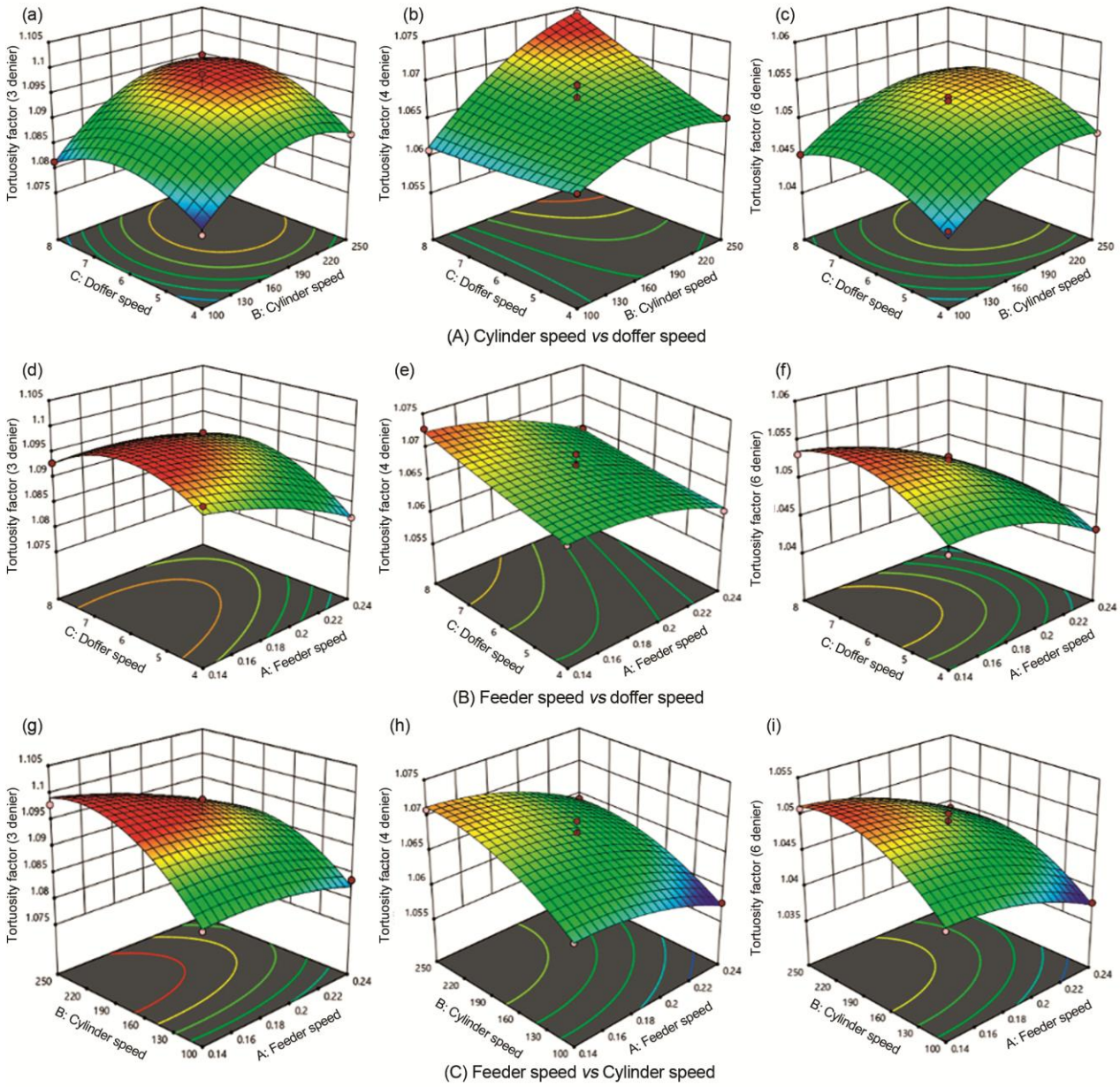

Fig. 6 — Tortuosity factor in nonwoven fabrics made from different denier fibres (A) - cylinder speed *vs* doffer speed (0.19 m/min feeder speed), (B) – feeder speed *vs* doffer speed (175 m/min cylinder speed), and (C) feeder speed *vs* cylinder speed (6 m/min doffer speed)

lower tortuosity values. The increased doffer speed notices an increase in tortuosity factor followed by a slight decrease towards higher doffer speed. The tortuosity factor observes an initial increase and then decrease with the increase in both feeder and doffer speeds. The increase in tortuosity factor is attributed to the combined effect of feeder and doffer which results in higher coefficient of relative fibre parallelisation and lower value of proportion of curved fibre ends. However, towards higher feeder and doffer speeds, the chances of hook formation increase, which causes poor fibre orientation. This is supported by the corresponding values of structural parameters as previously discussed. It is observed that the increase in fibre denier reduces the tortuosity factor due to same reasons as discussed above.

Figures 6 (g) - (i) show the 3D surface plots of feeder speed *vs*cylinder speed at constant doffer speed in relation to tortuosity factor in nonwoven fabric made from the fibre of different deniers. The 3D surface plots record an initial increase in the tortuosity factor with increased cylinder speed followed by a

decrease towards higher speeds. Similar trends are followed by all three deniers, but 6 denier fibres notice a slight decrease towards higher cylinder speed. As discussed above, an increase in cylinder speed induces improved orientation of fibres. However, towards higher cylinder speeds, there are chances of hook formation and fibre disorientation due to over-processing of the fibres. Further results indicate an increase followed by a decrease in tortuosity factor with the increase in feeder speed. The leading hooks created by the feeder speed are taken care of by the cylinder speed. Hence, the fibres get better oriented. However, further increase in cylinder and doffer speeds increase the chances of hook formation and fibre disorientation due to unfavourable speed ratios. An increase in both cylinder and feeder speeds reveals an increase and then a decrease in the tortuosity factor. This is attributed to the same reasons as discussed above. The tortuosity factor notices a decrease with an increase in fibre denier.

4 Conclusion

The proposed study provides an insight into the dual benefits of modulating the structure of nonwovens made of different deniers of fibre induced by optimised carding parameters for the enhancement of functional properties of needle-punched nonwovens. The orientation of carded web as characterised byproportion of curved fibre ends, coefficient of relative fibre parallelisation and anisotropy of inclination angle of fibres are highly influenced by considered carding parameters. It is concluded that, tortuosity factor is highly influenced by measured values of proportion of curved fibre ends, coefficient of relative fibre parallelisation, anisotropy of fibre inclination angle, fibre diameter and mean flow pore size. Accordingly, a nonlinear regression equation has been proposed, which establishes the tortuosity factor as a function of measured structural and physical characteristics of nonwoven, having R^2 value of 0.94 to calculate the tortuosity factor.

References

1 Anandjiwala R D & Boguslavsky L, *Text Res J*, 78 (2008) 614.
2 Yousfani S H S, Gong R H & Porat I, *Polym Compos*, 24 (2016) 65.
3 Saleh S S, *Am J Sci*, 8 (2012) 110.
4 Kothari V K, Das A & Sarkar A, *Indian J Fibre Text Res*, 32 (2007) 196.
5 Dixit P, Ishtiaque S M & Roy R, *Compos B Eng*, 182 (2020) 107654.
6 Chatterjee K N, Mukhopadhyay A, Jhalani G C & Mani B P, *Indian J Fibre Text Res*, 21 (1996) 251.
7 Chatterjee K N, Mukhopadhyay A, Jhalani G C & Mani B P, *Indian J Fibre Text Res*, 22 (1997) 13.
8 Chatterjee K N, Mukhopadhyay A, Jhalani G C & Mani B P, *Indian J Fibre Text Res*, 22 (1997) 21.
9 Lamb G E R, Miller B & Constanza P, *Text Res J*, 45 (1975) 452.
10 Das D, Das S & Ishtiaque S M, *Fibers Polym*, 15 (2014) 1456.
11 Pradhan A K, Das D & Chattopadhyay R, *J Ind Text*, 45 (2016) 1308.
12 Rashid M M, Motaleb A & Khan A, *J Eng Fibers Fabr*, 14 (2019) 1.
13 Ishtiaque S M, Choudhuria S & Das A, *Indian J Fibre Text Res*, 28 (2003) 405.
14 Ishtiaque S M, Mukhopadhyay A & Kumar A, *J Text Inst*, 99 (2008) 533.
15 Garde A R, Wakankar V A & Bhaduri S N, *Text Res J*, 31 (1961) 1026.
16 Jabbar A, Hussain T & Moqeet A, *J Eng Fibers Fabric*, 8 (2013).
17 Neckar B & Das D, *J Text Inst*, 103 (2012) 330.
18 Roy R & Ishtiaque S M, *Fibers Polym*, 20 (2019) 191.
19 Roy R & Ishtiaque S M, *Indian J Fibre Text Res*, 44 (2019) 131.
20 Roy R, Ishtiaque S M & Dixit P, *J Ind Text.* DOI: 10.1177/1528083720910706.
21 Roy R & Ishtiaque S M, *Indian J Fibre Text Res*, 44 (2019) 321.
22 Lindsley C H, *Text Res J*, 21 (1951) 39.
23 Leon'teva IS, *Technol Text Industry USSR*, 2 (1964) 57.
24 Vallabh R, Seyam A F, Banks-Lee P & Ducoste J, *Proceedings of the 6th World Conference on 3D Fabrics and their Applications*, Raleigh, NC, USA (2015).
25 Vallabh R, Ducoste J, Seyam A F & Banks-Lee P, *J Porous Media*, 14 (2011) 791.
26 Vallabh R, Banks-Lee P & Seyam A F, *J Eng Fibres Fabric*, 5 (2010) 7